

LETTERS

Preparation and detection of a mechanical resonator near the ground state of motion

T. Rocheleau^{1*}, T. Ndukum^{1*}, C. Macklin¹, J. B. Hertzberg², A. A. Clerk³ & K. C. Schwab⁴

Cold, macroscopic mechanical systems are expected to behave contrary to our usual classical understanding of reality; the most striking and counterintuitive predictions involve the existence of states in which the mechanical system is located in two places simultaneously. Various schemes have been proposed to generate and detect such states^{1,2}, and all require starting from mechanical states that are close to the lowest energy eigenstate, the mechanical ground state. Here we report the cooling of the motion of a radio-frequency nanomechanical resonator by parametric coupling to a driven, microwave-frequency superconducting resonator. Starting from a thermal occupation of 480 quanta, we have observed occupation factors as low as 3.8 ± 1.3 and expect the mechanical resonator to be found with probability 0.21 in the quantum ground state of motion. Further cooling is limited by random excitation of the microwave resonator and heating of the dissipative mechanical bath. This level of cooling is expected to make possible a series of fundamental quantum mechanical observations including direct measurement of the Heisenberg uncertainty principle and quantum entanglement with qubits.

Naively treating the motion of a mechanical resonator quantum mechanically produces the elementary result that the energy should be quantized: $E_n = \hbar\omega_m(n + 1/2)$, where n is an integer, ω_m is the resonant frequency (m denoting the mechanical resonator) and \hbar is Planck's constant divided by 2π . In thermal equilibrium, an average occupation factor is expected to follow the Bose–Einstein distribution: $\bar{n}_m^T = (e^{\hbar\omega_m/k_B T} - 1)^{-1}$, where T and k_B are the temperature and Boltzmann's constant, respectively. Cooling a resonator into the quantum regime where $\bar{n}_m^T \ll 1$, and measuring the very small motions, has been challenging for a number of technical reasons; not only are very low temperatures necessary to freeze out the mode, but detection with sensitivity at the quantum zero-point level, that is, on length scales $x_{zp} = \sqrt{\hbar/2m\omega_m}$, is required. Furthermore, this strong position measurement must not heat the mode with measurement back-action³.

Many strategies have been proposed^{4–8} and applied to realize the quantum regime, with increasing success. Experiments with nanoelectromechanical structures have been able to reach a mechanical occupation of $\bar{n}_m = 25$ by passively cooling a nanomechanical resonator³, detected with a superconducting single-electron transistor. (The mechanical occupation is not necessarily in equilibrium with the thermal occupation, \bar{n}_m^T .) Researchers experimenting with optomechanical systems have been able to use extremely sensitive optical detection and radiation pressure to both cool and detect $\bar{n}_m = 65$ in a toroidal resonator⁹, $\bar{n}_m = 37$ in microsphere resonator¹⁰ and $\bar{n}_m = 35$ in an optical cavity¹¹.

The technique we use to both cool and detect the motion of a nanomechanical resonator close to the ground state involves parametrically coupling the motion to a superconducting microwave

resonator (SMR)^{12,13} (Fig. 1). The nanomechanical resonator has a fundamental in-plane flexural resonance of $\omega_m = 2\pi \times 6.3$ MHz and is capacitively coupled to a symmetric, two-port, half-wave SMR that resonates at $\omega_{\text{SMR}} = 2\pi \times 7.5$ GHz. The device is located in a dilution refrigerator and pumped through carefully filtered and cooled leads. The thermal occupation of the SMR, \bar{n}_{SMR}^T , is expected to be 0.09 at 146 mK.

The nanomechanical-resonator damping rate, Γ_m^T , has an unusual linear temperature dependence below 600 mK, reaching a resonator quality factor of $Q \approx 10^6$ at 100 mK. The SMR damping rate, $\kappa = 2\pi \times 600$ kHz, is essentially temperature independent below 700 mK and is a factor of 2.4 higher than expected from design owing to internal losses.

The Hamiltonian that describes the coupled resonators is given by^{7,8}

$$\hat{H} = \hbar \left(\omega_{\text{SMR}} + g\hat{x} - \frac{1}{2}\lambda\hat{x}^2 \right) \left(\hat{b}^\dagger\hat{b} + \frac{1}{2} \right) + \hbar\omega_m \left(\hat{a}^\dagger\hat{a} + \frac{1}{2} \right)$$

where \hat{a} and \hat{a}^\dagger are respectively the nanomechanical-resonator annihilation and creation operators, and \hat{b} and \hat{b}^\dagger are those of the SMR. The first term shows the ponderomotive-like coupling of the SMR's frequency to the mechanical motion: $\hat{x} = x_{zp}(\hat{a}^\dagger + \hat{a})$ and $g = \partial\omega_{\text{SMR}}/\partial x = (\omega_{\text{SMR}}/2C_t)(\partial C_g/\partial x)$, where $C_g(x) = 450 \pm 50$ aF is the coupling capacitance and $C_t = 260$ fF is the SMR's total effective capacitance. The term proportional to \hat{x}^2 results from the electrostatic frequency-pulling of the mechanical resonator by the SMR¹⁴, where $\lambda = (\omega_{\text{SMR}}/2C_t)(\partial^2 C_g/\partial x^2)$, and is responsible for parametric instabilities under certain pump configurations.

When pumping the SMR at $\omega_p = \omega_{\text{SMR}} - \omega_m$ harmonic motion of the nanomechanical resonator preferentially up-converts microwave photons to frequency ω_{SMR} , extracting one radio-frequency nanomechanical-resonator quantum for each up-converted microwave SMR photon, a process that both damps and cools the nanomechanical resonator's motion^{7,8,15–17}. This cooling process is analogous to Raman scattering and the process used to cool an atomic ion to the quantum ground state of motion^{8,18}. In the sideband-resolved limit, $\kappa < \omega_m$ the rate of this up-conversion process is given by $\Gamma_{\text{opt}} \approx 4x_{zp}^2 g^2 \bar{n}_p / \kappa$, where \bar{n}_p is the occupation of the SMR resulting from the pumping.

From the detailed balance, the nanomechanical-resonator occupation factor is expected to follow

$$\bar{n}_m = \frac{\Gamma_m^T \bar{n}_m^T + \Gamma_{\text{opt}} \bar{n}_{\text{SMR}}}{\Gamma_m^T + \Gamma_{\text{opt}}} \quad (1)$$

where $\bar{n}_{\text{SMR}} = (\kappa/4\omega_m)^2 + \bar{n}_{\text{SMR}}^T [1 + 2(\kappa/4\omega_m)^2]$ is the effective occupancy associated with the SMR's back-action when $\Gamma_{\text{opt}} < \kappa$ (ref. 19). The first term in the expression for \bar{n}_{SMR} is due to the

¹Department of Physics, Cornell University, Ithaca, New York 14853, USA. ²Department of Physics, University of Maryland, College Park, Maryland 20742, USA. ³Department of Physics, McGill University, Montreal, Quebec H3A 2T8, Canada. ⁴Applied Physics, Caltech, Pasadena, California 91125, USA.

*These authors contributed equally to this work.

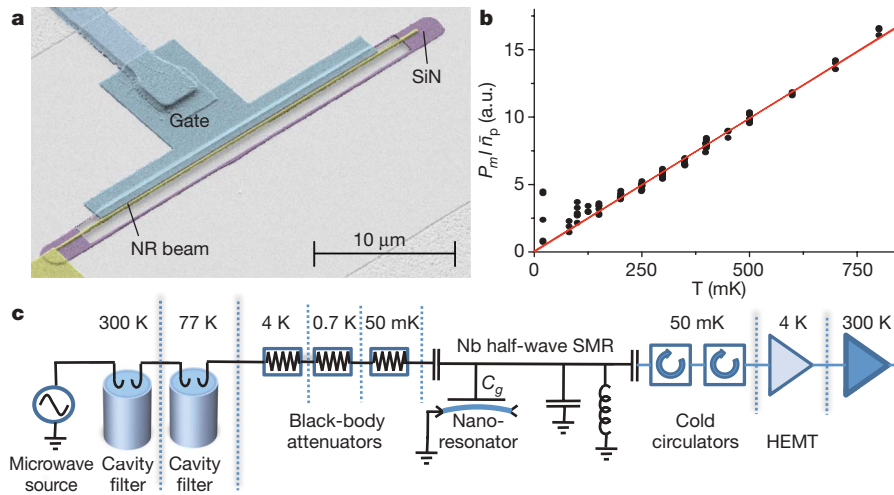


Figure 1 | Nanomechanical device, measurement diagram and thermal calibration. **a**, Nb–Al–SiN sample: the nanomechanical resonator is 30 μm long, 170 nm wide and 140 nm thick, is formed of 60 nm of stoichiometric, high-stress, low-pressure chemical-vapour-deposition SiN²⁹ and 80 nm of Al, and is located 75 nm from the gate electrode connected to the SMR. The SMR is made from a 345-nm-thick Nb film and has a waveguide

quantum fluctuations of the pump field, and the second term is due to the thermal occupation of the SMR, \bar{n}_{SMR}^T . The expressions above show that the minimum mechanical occupation possible is the effective occupation of the SMR.

The first realization of cooling in a parametrically coupled, electromechanical microwave system was with a kilogram-scale gravitational wave transducer²⁰, cooling from $\bar{n}_m = 10^8$ to $\bar{n}_m = 10^5$. Cooling of a nanomechanical resonator with an SMR was recently demonstrated²¹ and achieved cooling from $\bar{n}_m = 700$ to $\bar{n}_m = 120$ using a scheme similar to that presented here. Our results are made possible by improvements in device engineering (the coupling strength between the nanomechanical resonator and the SMR, g ; and the maximum SMR occupation, \bar{n}_{SMR}), which leads to an improvement in Γ_{opt} and resulting cooling rates of two orders of magnitude.

The up-converted noise power is calibrated by applying a weak pump signal ($\Gamma_{\text{opt}} < \Gamma_m^T$) and measuring the resulting integrated sideband power, P_m , normalized by the applied microwave pump power, \bar{n}_p , as a function of refrigerator temperature, T (Fig. 1b). For temperatures above ~ 150 mK, we observe the expected behaviour consistent with equipartition and use this curve to establish the relationship between measured output noise power and \bar{n}_m . For temperatures below 150 mK, we observe fluctuations in \bar{n}_m apparently due to a non-thermal, intermittent force noise at the level of 10^{-18} N Hz^{-1/2}, which is observed in other similar samples²² and is similar to anomalous heating effects in other systems²³. Furthermore, the linear temperature dependence of Γ_m^T causes the nanomechanical resonator to decouple from the thermal environment at the lowest measured temperatures. Although the behaviour of the nanomechanics seems consistent with a non-thermal force, we do not currently understand its source.

The measured signal powers are consistent with our knowledge of the attenuation and gain of our measurement circuit and estimates of the device parameters. We find that $g/2\pi = 84 \pm 5$ kHz nm⁻¹, which is the largest coupling strength so far demonstrated in a system of this type. From measurements of ω_m versus \bar{n}_p and pump frequency, we determine that $\lambda/2\pi = 2.1 \pm 0.7$ kHz nm⁻².

With the refrigerator stabilized at $T = 146$ mK ($\bar{n}_m^T = 480$), we measure output noise spectra, $S_x(\omega)$, versus the SMR pump occupation, \bar{n}_p . $S_x(\omega)$ is referred to the oscillator position using the nanomechanical-resonator thermal noise calibration, and is composed of up-converted microwave photons due to \bar{n}_m , SMR noise due to \bar{n}_{SMR} , and HEMT

characteristic impedance of 126 Ω . **b**, Thermal calibration of the up-converted noise power. **c**, Ultralow-noise, cryogenic measurement circuit with the SMR shown schematically as an equivalent inductance and capacitance. NR, nanomechanical resonator; HEMT, high-electron-mobility transistor; a.u., arbitrary units.

amplifier noise. We measure \bar{n}_{SMR} directly by observing the noise spanning the SMR resonance. Back-action correlations between the nanomechanical-resonator motion and the SMR field are important in our measured noise spectra at the lowest mechanical occupation factors. Fluctuations in the SMR voltage, due to \bar{n}_{SMR} , together with the pump, produce forces at frequency ω_m . The resulting motion, together with the pump, produces noise at frequency ω_{SMR} , but 180° out of phase with the original SMR fluctuations. This correlation results in an inverted noise peak, similar to noise squashing²⁴, which adds incoherently to the noise power driven by the thermal bath. The resulting observed noise peak or dip, \bar{n}_{eff} , is calibrated using thermal noise. Our analysis shows that the nanomechanical resonator occupation factor is given by $\bar{n}_m = \bar{n}_{\text{eff}} + 2\bar{n}_{\text{SMR}}$ (Supplementary Information). Figure 2 shows measurements of $S_x(\omega)$ in three cases at low occupation factors: $\bar{n}_{\text{eff}} > 0$, $\bar{n}_{\text{eff}} \approx 0$ and, showing the squashed output noise, $\bar{n}_{\text{eff}} < 0$.

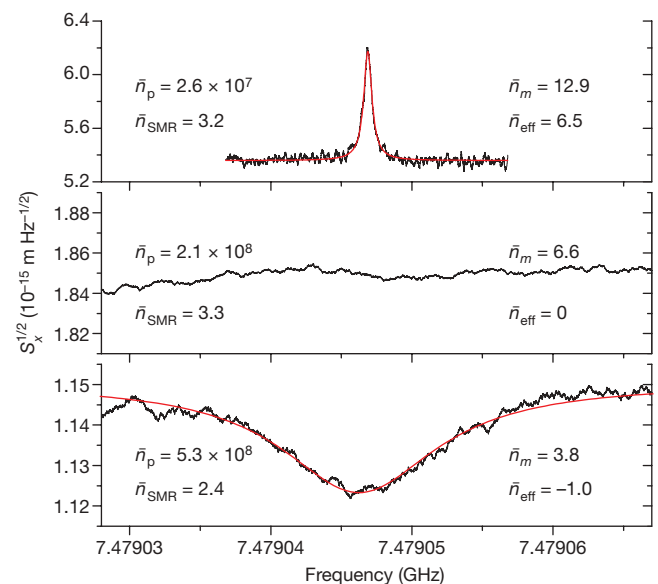


Figure 2 | Measured noise spectra. The noise squashing effect on $S_x(\omega)$ due to the finite occupation of the SMR can be seen in three situations: $\bar{n}_{\text{eff}} > 0$ (top), $\bar{n}_{\text{eff}} \approx 0$ (middle) and $\bar{n}_{\text{eff}} < 0$ (bottom). The red curves show Lorentzian fits through the mechanically up-converted sideband.

Taking the effects of \bar{n}_{SMR} into account in this way, the lowest mechanical occupation we have observed is $\bar{n}_m = 3.8 \pm 1.3$, shown in Fig. 2, with the uncertainty dominated by the uncertainty in \bar{n}_{SMR} . At this low occupation factor, the resonator is expected to be found in the ground state with probability $P_0 = 1/(\bar{n}_m + 1) = 0.21$. The cooling power of this refrigeration technique is $\dot{Q} = \hbar\omega_m\Gamma_{\text{opt}} = 10^{-22}$ W.

We lowered the refrigerator temperature to 20 mK and did not observe a decrease in the minimum \bar{n}_m value. Using the detailed balance relationship and the measured values of \bar{n}_m , \bar{n}_{SMR} and Γ_{opt} values, we can compute the bath heating rate, $\dot{n}_T = \Gamma_m^T \bar{n}_m^T$, as a function of \bar{n}_p (Fig. 3). It is clear that as \bar{n}_p increases above 3×10^7 , \dot{n}_T begins to increase, nullifying the benefit of starting at low temperatures. This level of heating is consistent with ohmic losses in the metal film on top of the nanomechanical resonator, and the thermal conductance of a normal-state electron gas.

To check the behaviour of our system (nanomechanical resonator and SMR) in a range where \bar{n}_{SMR}^T is not a complicating factor, we applied radio-frequency electrostatic force noise at the nanomechanical-resonator frequency. Starting from $\bar{n}_m = 2.5 \times 10^5$, we observe cooling, by a factor of 3,000, to $\bar{n}_m = 80$, which closely follows the expected cooling curve over the full range of \bar{n}_p (Fig. 4). This suggests that the increase in bath rate at high pump power is due primarily to an increase in bath temperature and not a significant increase in Γ_m^T . To check the stability of our system, we cycled the device from millikelvin temperatures to 77 K and back. To within a few per cent, we observed no change in the microwave signal levels generated by thermal noise, and no change in Γ_{opt} as a function of \bar{n}_p . We also found the out-of-plane mechanical resonance to be 150 kHz lower than the in-plane resonance used in this work. This additional resonance is sufficiently different in frequency that we do not expect any significant interaction.

These measurements identify three effects that work against the cooling process: excess fluctuations of the SMR (\bar{n}_{SMR}), heating of the nanomechanical resonator thermal bath at high pump powers, and the non-thermal force noise at low temperatures.

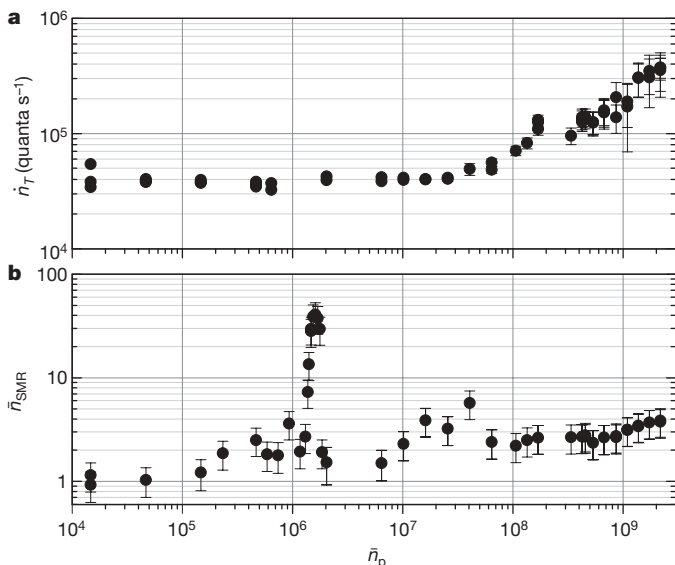


Figure 3 | Nanomechanical heating rate and superconducting-resonator occupation versus pump strength. **a**, The upper figure shows the bath heating rate, \dot{n}_T , and the onset of excess heating above $\bar{n}_p = 3 \times 10^7$. **b**, The lower figure shows the measured value of thermal occupation of the SMR; the structure is suspected to be related to temporal dynamics of the transition between superconducting and normal states of the metal films and resulting microwave sideband generation³⁰. The error bars on \bar{n}_{SMR} (s.e.m.) are dominated by the uncertainty in the transmission of our microwave circuit: gain of our HEMT amplifier and attenuation of our microwave cables and isolators. The error bars on \dot{n}_T (s.e.m.) result from standard error propagation in equation (1) and are dominated by the uncertainty in \bar{n}_{SMR} .

We believe that the excess SMR occupation, \bar{n}_{SMR} , is not a result of phase or amplitude noise of our microwave source: the pump signal is filtered using tunable, copper microwave cavities (one at 300 K ($Q = 9.5 \times 10^3$) and a second at 77 K ($Q = 2.6 \times 10^4$)) achieving a noise power measured 6.3 MHz from, and relative to, ω_p of less than $-195 \text{ dB}_c \text{ Hz}^{-1}$ (where dB_c denotes units of noise power measured relative to the pump power) and contributing less than 0.04 photons into the SMR at our highest value of \bar{n}_p . Without these cavities, the SMR would be excited to $\bar{n}_{\text{SMR}} = 35$. We also believe that this excess SMR occupation is not due to ohmic heating of, and resulting thermal radiation from, the cryogenic attenuator network because \bar{n}_{SMR} increases only weakly over a wide range of \bar{n}_p values. Tests of Nb SMR devices at 1.2 K before the surface micromachining of the nanomechanical resonator do not show excess dissipation and suggest that the excess losses are related to our fabrication process.

Increasing Γ_{opt} by engineering a larger coupling strength, g , and/or a smaller κ value should be very beneficial as it will lead to higher cooling rates at lower pump powers, minimizing the effect of excess bath heating, \dot{n}_T . By increasing Γ_{opt} by a factor of ten, maintaining the same value of \dot{n}_T , we expect to obtain $\bar{n}_m \approx 0.5$ with $P_0 = 0.67$. This approach will be limited when Γ_{opt} becomes comparable to κ , which constrains the rate of cooling^{19,25}.

The deep quantum limit, $\bar{n}_m \ll 1$, will be accessible when it is possible to reach lower refrigerator temperatures and lower mechanical

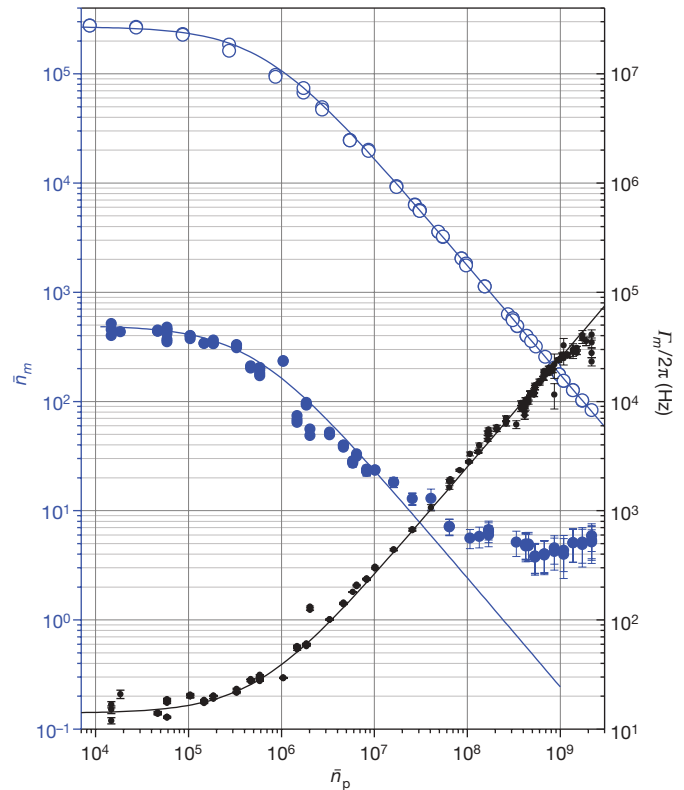


Figure 4 | Mechanical linewidth broadening and cooling versus pump strength. Mechanical occupation factor, \bar{n}_m (blue), and total mechanical linewidth, $\Gamma_m = \Gamma_m^T + \Gamma_{\text{opt}}$ (black), versus drive photon occupation, \bar{n}_p . The lower cooling curve starts from a refrigerator temperature of 146 mK, and the upper curve starts from an effective temperature of 80 K, which is generated by applying an electrostatic force noise to the nanomechanical resonator. The solid black curve is a fit to the measured Γ_m values. The solid blue curves are the expected values of \bar{n}_m assuming ideal values of \bar{n}_{SMR} and $\dot{n}_T = 4 \times 10^4$ quanta per second (filled points) and $\dot{n}_T = 2 \times 10^6$ quanta per second (open points). The error bars on Γ_m arise from the statistical fluctuations in our measured noise power and the resulting standard error in the Lorentzian fit parameters. The error bars on \bar{n}_m (s.e.m.) include the same source of statistical error, as well as the uncertainty in SMR occupation, which is calculated from best estimates of uncertainties in line loss and amplifier gain (Supplementary Information).

damping rates at these temperatures. Understanding and eliminating the excess bath heating and the non-thermal force noise will be required, although it should be pointed out that, even without these improvements, the device described here should achieve $\bar{n}_m < 0.5$ if excess SMR occupation is reduced. Furthermore, superconducting metals on the nanomechanical resonator also appear to be required owing to the expected mechanical force noise from transport and electron momentum scattering in diffusive conductors²⁶. For a normal-state conductor, each electron scattering event imparts a momentum change on the order of the Fermi momentum. The diffusive scattering of current through the beam directly produces force noise on the nanomechanical resonator. We estimate that this heating mechanism will result in a limit of $\bar{n}_m > 3$ at $\bar{n}_p = 3 \times 10^8$, assuming our current device parameters and a resistance of 100 Ω through the nanomechanical resonator.

These measurements show that detection with sensitivity to resolve motions approaching the ground state is possible with existing HEMT-based amplifiers. Eliminating internal SMR losses, unbalancing the SMR couplings and using improved microwave amplifiers²⁷ would significantly reduce the measurement time.

Nonetheless, the production and detection of a nanomechanical resonator with $\bar{n}_m = 3.8$ is sufficient to allow future experiments. Owing to uncertainty-principle fluctuations of the mechanical motion, and resulting spontaneous emission, the rate of microwave-photon up-conversion is expected to differ from the rate of down-conversion. This difference can be used as a fundamental thermometry technique^{7,8,18}, and would allow the quantitative measurement of the zero-point motion of a mechanical structure.

This level of cooling is essential for the formation of entangled states between superconducting quantum bits and the motion of a nanomechanical device. Proposed schemes^{1,28} allow the generation and detection of nanomechanical resonator/qubit entanglement using a Jaynes–Cummings-type interaction with the mechanical resonator at thermal occupations of the level shown here. Similar to procedures in atomic physics, such an experiment would involve preparing the cold state of the mechanical device and, after the refrigeration is complete, turning the cooling off. The state of the cold beam could then be manipulated before thermalization of the motion. In our implementation of this process, we expect cooling from $\bar{n}_m = 500$ to $\bar{n}_m = 4$ in $\sim 200 \mu\text{s}$, and we expect one thermal quantum to enter the resonator in $\tau = 1/\hbar_T = 2 \mu\text{s}$, which exceeds superconducting qubit manipulation times and is comparable to qubit measurement and relaxation times.

Received 13 August; accepted 18 November 2009.
Published online 9 December 2009.

1. Armour, A., Blencowe, M. & Schwab, K. Entanglement and decoherence of a micromechanical resonator via coupling to a Cooper-pair box. *Phys. Rev. Lett.* **88**, 148301 (2002).
2. Marshall, W., Simon, C., Penrose, R. & Bouwmeester, D. Towards quantum superposition of a mirror. *Phys. Rev. Lett.* **91**, 130401 (2003).
3. Naik, A. *et al.* Cooling a nanomechanical resonator with quantum back-action. *Nature* **443**, 193–196 (2006).
4. Courty, J. M., Heidmann, A. & Pinard, M. Quantum limits of cold damping with optomechanical coupling. *Eur. Phys. J. D* **17**, 399–408 (2001).
5. Martin, I., Shnirman, A., Tian, L. & Zoller, P. Ground-state cooling of mechanical resonators. *Phys. Rev. B* **69**, 125339 (2004).
6. Blencowe, M. P. & Buks, E. Quantum analysis of a linear dc SQUID mechanical displacement detector. *Phys. Rev. B* **76**, 014511 (2007).
7. Marquardt, F., Chen, J. P., Clerk, A. A. & Girvin, S. M. Quantum theory of cavity-assisted sideband cooling of mechanical motion. *Phys. Rev. Lett.* **99**, 093902 (2007).
8. Wilson-Rae, I., Nooshi, N., Zwinger, W. & Kippenberg, T. J. Theory of ground state cooling of a mechanical oscillator using dynamical backaction. *Phys. Rev. Lett.* **99**, 093901 (2007).

9. Schliesser, A., Arcizet, O., Riviere, R., Anetsberger, G. & Kippenberg, T. J. Resolved-sideband cooling and position measurement of a micromechanical oscillator close to the Heisenberg uncertainty limit. *Nature Phys.* **5**, 509–514 (2009).
10. Park, Y.-S. & Wang, H. Resolved-sideband and cryogenic cooling of an optomechanical resonator. *Nature Phys.* **5**, 489–493 (2009).
11. Groblacher, S. *et al.* Demonstration of an ultracold micro-optomechanical oscillator in a cryogenic cavity. *Nature Phys.* **5**, 485–488 (2009).
12. Day, P. K., LeDuc, H. G., Mazin, B. A., Vayonakis, A. & Zmuidzinas, J. A broadband superconducting detector suitable for use in large arrays. *Nature* **425**, 817–821 (2003).
13. Regal, C. A., Teufel, J. D. & Lehnert, K. W. Measuring nanomechanical motion with a microwave cavity interferometer. *Nature Phys.* **4**, 555–560 (2008).
14. Cleland, A. N. & Roukes, M. L. A nanometre-scale mechanical electrometer. *Nature* **392**, 160–162 (1998).
15. Dykman, M. I. Heating and cooling of local and quasilocal vibrations by nonresonant eld. *Sov. Phys. Solid State* **20**, 1306 (1978).
16. Linthorne, N. P., Veitch, P. J. & Blair, D. G. Interaction of a parametric transducer with a resonant bar gravitational radiation detector. *J. Phys. D* **23**, 1–6 (1990).
17. Xue, F., Wang, Y. D., Liu, Y.-X. & Nori, F. Cooling a micromechanical beam by coupling it to a transmission line. *Phys. Rev. B* **76**, 205302 (2007).
18. Diedrich, F., Bergquist, J. C., Itano, W. & Wineland, D. J. Laser cooling to the zero-point energy of motion. *Phys. Rev. Lett.* **62**, 403–406 (1989).
19. Dobrindt, J. M., Wilson-Rae, I. & Kippenberg, T. J. Parametric normal-mode splitting in cavity optomechanics. *Phys. Rev. Lett.* **101**, 263602 (2008).
20. Blair, D. G. *et al.* High sensitivity gravitational wave antenna with parametric transducer readout. *Phys. Rev. Lett.* **74**, 1908–1911 (1995).
21. Teufel, J. D., Harlow, J. W., Regal, C. A. & Lehnert, K. W. Dynamical backaction of microwave fields on a nanomechanical oscillator. *Phys. Rev. Lett.* **101**, 197203 (2008).
22. Teufel, J. D., Regal, C. A. & Lehnert, K. W. Prospects for cooling nanomechanical motion by coupling to a superconducting microwave resonator. *New J. Phys.* **10**, 095002 (2008).
23. Stipe, B. C., Mamin, H. J., Stowe, T. D., Kenny, T. W. & Rugar, D. Noncontact friction and force fluctuations between closely spaced bodies. *Phys. Rev. Lett.* **87**, 096801 (2001).
24. Poggio, M., Degen, C. L., Mamin, H. J. & Rugar, D. Feedback cooling of a cantilever's fundamental mode below 5mk. *Phys. Rev. Lett.* **99**, 017201 (2007).
25. Grajcar, M., Ashhab, S., Johansson, J. R. & Nori, F. Lower limit on the achievable temperature in resonator-based sideband cooling. *Phys. Rev. B* **78**, 035406 (2008).
26. Shytov, A. V., Levitov, L. S. & Beenakker, C. W. J. Electromechanical noise in a diffusive conductor. *Phys. Rev. Lett.* **88**, 228303 (2002).
27. Castellanos-Beltran, M. A., Irwin, K. D., Hilton, G. C., Vale, L. R. & Lehnert, K. W. Amplification and squeezing of quantum noise with a tunable Josephson metamaterial. *Nature Phys.* **4**, 929–931 (2008).
28. Utami, D. W. & Clerk, A. A. Entanglement dynamics in a dispersively coupled qubit-oscillator system. *Phys. Rev. A* **78**, 042323 (2008).
29. Verbridge, S. S., Craighead, H. G. & Parpia, J. M. A megahertz nanomechanical resonator with room temperature quality factor over a million. *Appl. Phys. Lett.* **92**, 013112 (2008).
30. Segev, E., Abdo, B., Shtempluck, O. & Buks, E. Thermal instability and self-sustained modulation in superconducting NbN stripline resonators. *J. Phys. Condens. Matter* **19**, 096206 (2007).

Supplementary Information is linked to the online version of the paper at www.nature.com/nature.

Acknowledgements We acknowledge conversations with M. Blencowe, M. Aspelmeyer, R. Ilic, M. Skvarla, M. Metzler and M. Shaw and assistance from M. Savva, S. Rosenthal and M. Corbett. This work has been supported by the Fundamental Questions Institute (<http://fqxi.org>) (RFP2-08-27) and the US National Science Foundation (NSF) (DMR-0804567). Device fabrication was performed at the Cornell Nanoscale Facility, a member of the US National Nanotechnology Infrastructure Network (NSF grant ECS-0335765).

Author Contributions T.R. and T.N. contributed equally to device fabrication and measurements. C.M. built key apparatus and assisted in experimental set-up. J.B.H. assisted in planning and analysis. A.A.C. provided theoretical analysis. K.C.S. initiated and oversaw the work.

Author Information Reprints and permissions information is available at www.nature.com/reprints. The authors declare no competing financial interests. Correspondence and requests for materials should be addressed to K.C.S. (schwab@caltech.edu).